Low-Voltage, Low-Power, Organic Light-Emitting Transistors for Active Matrix Displays

M. A. McCarthy, *et al.*

Science **332**, 570 (2011);
DOI: 10.1126/science.1203052

The minimum energy per bit obtained with our sharpest (~20 ns) pulses is of the order ~100 fJ. However, the linear trend of V_T with nanogap size (Fig. 4B) reveals that such devices are highly scalable and suggests that ~5-nm GST bits with CNT electrodes could operate at ~0.5 V and <1 μA, such that nanosecond switching times (*29*, *30*) would lead to sub-femtojoule per bit energy consumption [for additional estimates see section 6 of (*19*)]. Low-voltage operation could also be achieved by using materials with lower threshold fields, such as GeSb (*27*). These results are encouraging for ultralow-power electronics and memory based on programmable PCM with nanoscale carbon interconnects.

References and Notes

1. M. Wuttig, N. Yamada, *Nat. Mater.* **6**, 824 (2007).
2. A. V. Kolobov *et al.*, *Nat. Mater.* **3**, 703 (2004).
3. H.-S. P. Wong *et al.*, *Proc. IEEE* **98**, 2201 (2010).
4. M. H. Lankhorst, B. W. Ketelaars, R. A. Wolters, *Nat. Mater.* **4**, 347 (2005).
5. K. N. Chen *et al.*, *IEEE Electron Device Lett.* **29**, 131 (2008).
6. S.-M. Yoon, S.-W. Jung, S.-Y. Lee, Y.-S. Park, B.-G. Yu, *IEEE Electron Device Lett.* **30**, 371 (2009).
7. G. W. Burr *et al.*, *J. Vac. Sci. Technol. B* **28**, 223 (2010).
8. S. Raoux, W. Wełnic, D. Ielmini, *Chem. Rev.* **110**, 240 (2010).
9. S.-H. Lee, Y. Jung, R. Agarwal, *Nat. Nanotechnol.* **2**, 626 (2007).
10. D. Yu, S. Brittman, J. S. Lee, A. L. Falk, H. Park, *Nano Lett.* **8**, 3429 (2008).
11. S. Meister, D. T. Schoen, M. A. Topinka, A. M. Minor, Y. Cui, *Nano Lett.* **8**, 4562 (2008).
12. Y. C. Chen *et al.*, in *International Electron Devices Meeting 2006 (IEDM)* (IEEE, Piscataway, NJ, 2006); 10.1109/IEDM.2006.346910.
13. J. I. Lee *et al.*, in *2007 IEEE Symposium on VLSI Technology* (IEEE, Piscataway, NJ, 2007), pp. 102–103, 10.1109/VLSIT.2007.4339744.
14. D. H. Im *et al.*, in *International Electron Devices Meeting 2008 (IEDM)* (IEEE, Piscataway, NJ, 2008); 10.1109/IEDM.2008.4796654.
15. P. Qi *et al.*, *J. Am. Chem. Soc.* **126**, 11774 (2004).
16. C. M. Aguirre, C. Ternon, M. Paillet, P. Desjardins, R. Martel, *Nano Lett.* **9**, 1457 (2009).
17. A. Liao, Y. Zhao, E. Pop, *Phys. Rev. Lett.* **101**, 256804 (2008).
18. F. Xiong, A. Liao, E. Pop, *Appl. Phys. Lett.* **95**, 243103 (2009).
19. Additional experimental data and simulations are available as supporting materials on *Science* Online.
20. A. Liao *et al.*, *Phys. Rev. B* **82**, 205406 (2010).
21. E. Pop, D. A. Mann, K. E. Goodson, H. J. Dai, *J. Appl. Phys.* **101**, 093710 (2007).
22. Because the entire device is covered by a-GST, R_{OFF} is limited by (small) leakage between the metal electrodes.
23. D. Ielmini, Y. Zhang, *J. Appl. Phys.* **102**, 054517 (2007).
24. A. Redaelli *et al.*, *IEEE Electron Device Lett.* **25**, 684 (2004).
25. V. G. Karpov, Y. A. Kryukov, I. V. Karpov, M. Mitra, *Phys. Rev. B* **78**, 052201 (2008).
26. I. R. Chen, E. Pop, *IEEE Trans. Electron. Dev.* **56**, 1523 (2009).
27. D. Krebs *et al.*, *Appl. Phys. Lett.* **95**, 082101 (2009).
28. J. Yao *et al.*, *Small* **5**, 2910 (2009).
29. G. Bruns *et al.*, *Appl. Phys. Lett.* **95**, 043108 (2009).
30. W. J. Wang *et al.*, *Appl. Phys. Lett.* **93**, 043121 (2008).

Acknowledgments: We acknowledge valuable discussions with J. Abelson and D. Ielmini. This work was supported in part by the Materials Structures and Devices (MSD) Focus Center, under the Focus Center Research Program (FCRP), a Semiconductor Research Corporation entity. Additional funding was provided by the Nanotechnology Research Initiative (NRI) Fellowship (A.L.), a NSF Graduate Fellowship (D.E.), and the Office of Naval Research (ONR).

Supporting Online Material

www.sciencemag.org/cgi/content/full/science.1201938/DC1
Materials and Methods
SOM Text
Figs. S1 to S9
References

20 December 2010; accepted 16 February 2011
Published online 10 March 2011;
10.1126/science.1201938

Low-Voltage, Low-Power, Organic Light-Emitting Transistors for Active Matrix Displays

M. A. McCarthy,[1,2] B. Liu,[1] E. P. Donoghue,[1] I. Kravchenko,[3] D. Y. Kim,[2] F. So,[2] A. G. Rinzler[1]*

Intrinsic nonuniformity in the polycrystalline-silicon backplane transistors of active matrix organic light-emitting diode displays severely limits display size. Organic semiconductors might provide an alternative, but their mobility remains too low to be useful in the conventional thin-film transistor design. Here we demonstrate an organic channel light-emitting transistor operating at low voltage, with low power dissipation, and high aperture ratio, in the three primary colors. The high level of performance is enabled by a single-wall carbon nanotube network source electrode that permits integration of the drive transistor and the light emitter into an efficient single stacked device. The performance demonstrated is comparable to that of polycrystalline-silicon backplane transistor-driven display pixels.

Organic light-emitting diode (OLED) displays have well-recognized advantages in power consumption, pixel brightness, viewing angle, response time, and contrast ratio over liquid crystal displays (LCDs) (*1*). The primary technical challenge preventing wider commercial implementation remains the drive transistor in the active matrix (AM) backplane. Amorphous silicon (a-Si), the transistor channel material that sources the voltage to switch AM-LCD pixels, has a low mobility (~1 $cm^2 V^{-1} s^{-1}$) (*2*). To drive the currents necessary for OLEDs would require higher drive voltages, consuming power; moreover, its stability is unacceptable for AMOLED pixels (*3*, *4*). For small AMOLED displays now in some handheld devices, the solution has been to use low-temperature polycrystalline silicon (poly-Si). However, poly-Si adds processing steps, time, and expense to the device fabrication (*5*, *6*). Poly-Si also suffers from a more fundamental limitation: variation in the size, orientation, and number of the large polycrystalline grains (important to its high mobility for sourcing the high drive currents) leads to pixel-to-pixel inhomogeneity (*7*). This limits the production yield and becomes an increasingly severe problem with increasing display size.

Organic semiconductor channel materials are attractive for their homogeneity, low cost, and the variety of means by which they can be deposited, but their best mobilities are similar to that of a-Si. In the typical thin-film transistor (TFT) architecture, low-mobility channel layers would require a large source-drain voltage to drive the necessary current. This consumes power in the transistor (as opposed to light production in the OLED), compromising the power savings. In one all-organic AMOLED demonstration, more power was dissipated in the drive transistor than in the OLED it was powering (*8*). Mitigating this by increasing the channel width of the drive transistor to source more current is not viable; to do so would reduce the fraction of pixel area available to the OLED, requiring a higher current density through the electroluminescent emitter to maintain the display brightness, reducing OLED lifetime (*9*). Alternatively, the low mobility of the organics could be compensated by making the channel length short, placing the source and drain terminals very close to each other; but that incurs the expense of high-resolution patterning.

We recently demonstrated a carbon nanotube enabled vertical field effect transistor (CN-VFET) that, intrinsic to its architecture, permits short channel lengths without high-resolution patterning and gave on-currents sufficient to drive OLED pixels at low operating voltages (*10*). Here, to realize the full benefit of the architecture, we integrate the OLED into the CN-VFET stack. We call such a device a carbon nanotube enabled vertical organic light-emitting transistor (CN-VOLET)

[1]Department of Physics, University of Florida, Gainesville, FL 32611, USA. [2]Department of Materials Science and Engineering, University of Florida, Gainesville, FL 32611, USA. [3]Center for Nanophase Materials Sciences, Oak Ridge National Laboratory, Oak Ridge, TN 37830, USA.

*To whom correspondence should be addressed. E-mail: rinzler@phys.ufl.edu

(*11*). Here red, green, and blue CN-VOLETs are demonstrated that take full advantage of the low power dissipation of the integrated drive transistor and, further, exploit the high transmittance of the nanotube source electrode—greater than 98% across the visible spectrum—to yield a light-emitting transistor that emits light across its full aperture.

Vertical-type organic light-emitting transistors (OLETs) of varied designs and operating principles have appeared in recent years (*12*–*18*). The best performance was demonstrated by Nakamura *et al*. (*18*) in an architecture designated a metal insulator semiconductor (MIS)–OLET. Their $Ir(ppy)_3$ emitter-based OLET possessed an effective aperture ratio (*19*) of 45% and achieved a brightness of 500 cd/m^2 at gate and drain voltages of −30 V and −13.3 V, respectively. For a typical $Ir(ppy)_3$ OLED to emit at this luminous flux through an aperture transmitting 45% of its light, the OLED would need to emit at 1100 cd/m^2, which would in turn require a cathode-anode voltage of approximately −6.5 V (*20*). This implies that −6.8 V of the −13.3 V drain voltage used by the MIS-OLET was dropped across its integrated "transistor" portion, which then dissipated 51% of the total power.

Our CN-VOLET can be thought of as an OLED stack inserted between the organic semiconductor of a CN-VFET and its drain electrode with the latter made an electron-injecting, low–work function metal (Fig. 1) (*10*, *11*). The CN-VFET substructure thus controls hole injection into the OLED layers. In the CN-VFET the nanotubes are spread as a dilute network, well above electrical percolation [image in fig. S1A and transmittance spectrum in fig. S1B (*21*)] across the gate dielectric sitting on a bottom gate electrode. A metal electrode provides electrical contact along one edge of the network. Because the nanotubes are used as the source electrode, rather than as the active channel, no separation of metallic from semiconducting nanotubes is necessary. The organic channel layer is deposited as a thin film across the nanotubes and the exposed dielectric, and finally, in the case of the CN-VFET, a metal drain electrode is deposited onto the organic channel layer, completing the device. The transconductance originates from a gate field–induced modulation of the Schottky barrier height and width between the nanotubes and the organic channel layer (*11*). Insertion of the OLED layers between the CN-VFET channel layer and the drain integrates the driving transistor and the light emitter in the single, stacked device. Because of the strong gate coupling to the nanotube source electrode, the Schottky barrier modulation alone is sufficient to turn the devices off without the need for an overlying insulator as required by the MIS-OLET (*18*) and responsible for limiting its aperture ratio. Combined with the high optical transmittance of the nanotube source electrode and a transparent indium tin oxide (ITO) gate, our bottom emitting devices radiate light across their full aperture.

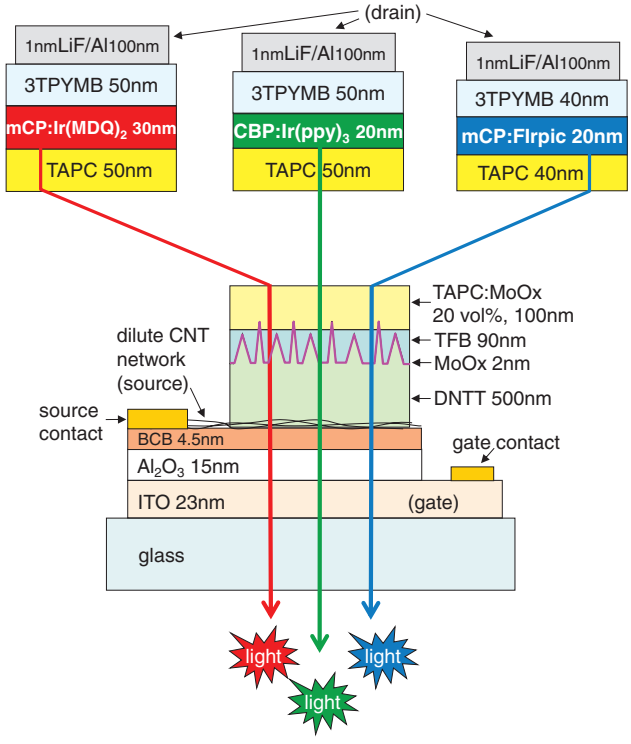

Fig. 1. Schematics of the red, green, and blue CN-VOLETs. The base of the device (i.e., the substrate, gate, source, and channel layers) is the same for each color device.

Figure 1 shows a schematic cross section of the CN-VOLET fabricated for each primary color. The material of each layer is listed in Table 1. The DNTT (*22*) organic channel layer, made thick to eliminate shorting paths from residual particulates in the carbon nanotube (CNT) source material, acquired a rough surface morphology (*23*) as indicated by the spikes in Fig. 1. Nontrivial planarization and strategic doping (*24*, *25*) were used to overcome the issues arising from this roughness. Complete fabrication details including extensive experiments required to overcome the CN-VFET substructure roughness are provided in (*21*).

In operation, the CNT source electrode was held at ground potential, and the drain and gate were biased relative to ground. Figure 2 plots the performance characteristics for each color device. Current density and luminance versus voltage (*J-L-V*) output curves (Fig. 2, A to C) and transfer curves (Fig. 2, D to F) are shown. Each color CN-VOLET operates at a gate voltage (V_G) range of ±3 V; the luminance surpasses 500 cd/m^2 at drain voltages (V_D) of −6.8 V (red), −4.9 V (green), −5.7 V (blue), with contrast ratios (ratio of the luminance at a given V_D between the on and off states) approaching 10^4. These voltages are well within the range of typical poly-Si–based AMOLEDs (*26*, *27*). Negligible hysteresis was observed in the dual scan direction transfer curves (Fig. 2, D to F) (*28*). The gate leakage current density (J_G) remains below the drain current density (J_D) by one order of magnitude or more in the off state (V_G = +3 V) and by three orders of magnitude or more in the on state (V_G = −3 V). Optical micrographs for each color (Fig.

Table 1. CN-VOLET organic layers chemical name and function.

Abbreviation	Chemical name	Function
DNTT	Dinaphtho-[2,3-*b*:2′,3′-*f*]thieno[3,2-*b*]-thiophene	High-mobility channel layer
TFB	Poly(9,9-dioctyl-fluorene-co-*N*-(4-butylphenyl)-diphenylamine)	Planarization channel layer
TAPC	1,1-Bis[(di-4-tolyamino)phenyl]cyclohexane	Hole transport layer
CBP	4,4-*N*,*N*-dicarbazole-biphenyl	Emitter host (green)
mCP	*N*,*N*′-Dicarbazolyl-3,5-benzene	Emitter host (red, blue)
$Ir(MDQ)_2$	Iridium(III)bis(2-methyldibenzo[*f*,*h*]quinoxaline)(acetylacetonate)	Red emitter
$Ir(ppy)_3$	*Fac*-tris(2-phenylpyridinato)iridium(III)	Green emitter
Firpic	Bis[(4,6-di-fluorophenyl)-pyridinate-*N*,C2′]picolinate	Blue emitter
3TPYMB	Tris[3-(3-pyridyl)-mesityl]borane	Electron transport layer

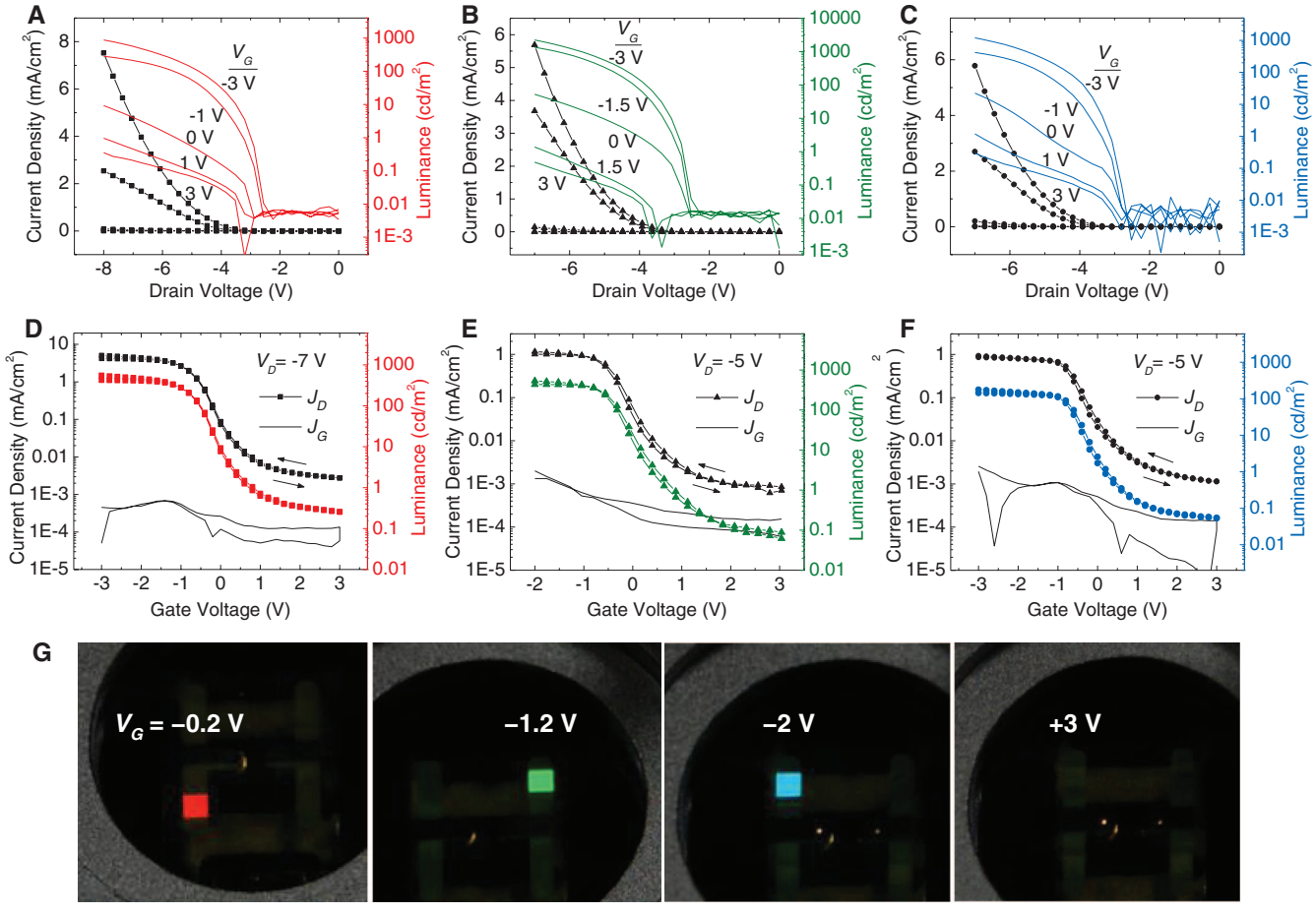

Fig. 2. CN-VOLET device operation. (**A** to **C**) Output and (**D** to **F**) transfer *J-L-V* curves of the (A and D) red, (B and E) green, and (C and F) blue CN-VOLETs. (**G**) Images of the corresponding color CN-VOLET pixels (1 mm by 1 mm) below the graphs, at the indicated gate voltage. The diameter of the fixture opening is 14 mm. In the far right image, the blue CN-VOLET was in the fully off state (i.e., V_G = +3 V), which is also representative of the red and green CN-VOLETs in the off state.

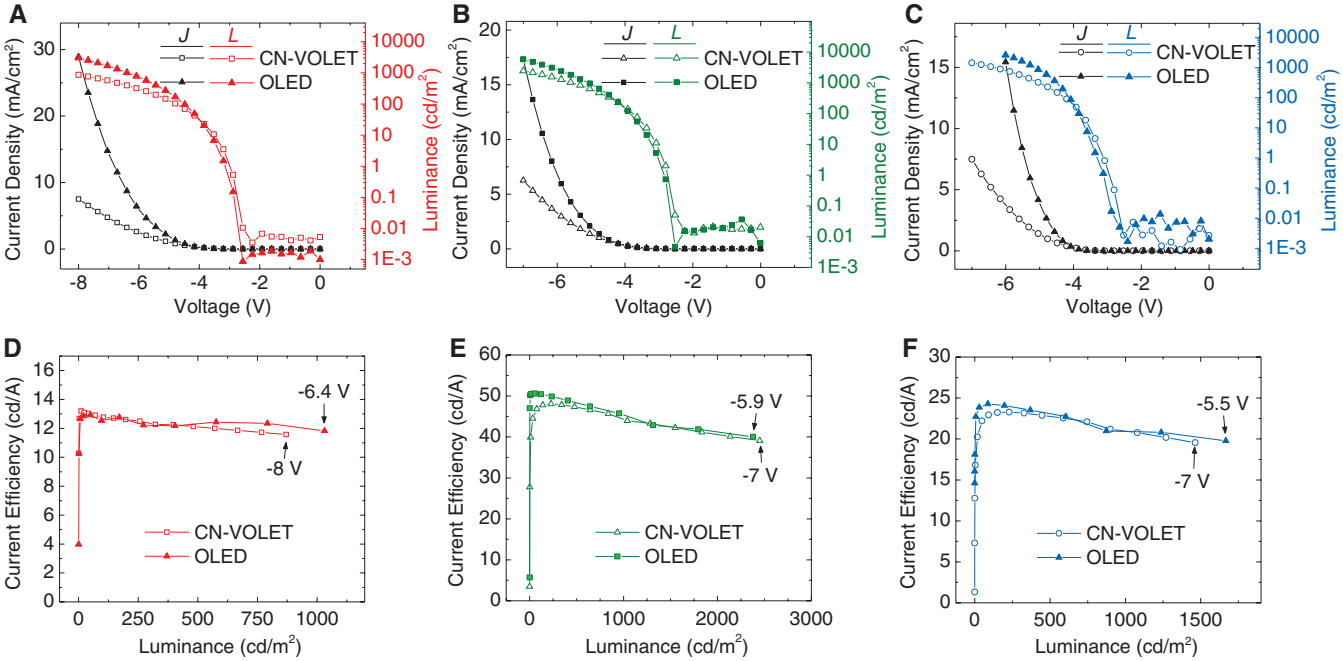

Fig. 3. Comparison of the CN-VOLETs to control OLEDs. *J-L-V* comparison for the (**A**) red, (**B**) green, and (**C**) blue CN-VOLETs in the on state (i.e., V_G = −3 V) to their respective OLEDs. Applied voltage is on the drain of the CN-VOLET (source grounded) and on the cathode (anode grounded) of the OLED. Comparison of current efficiencies of (**D**) red, (**E**) green, and (**F**) blue CN-VOLETs (V_G = −3 V) to their respective OLEDs. Negligible light is absorbed and/or scattered in the base layers of the CN-VOLET.

Table 2. Turn-on voltages (*29*) and current efficiencies of red, green, and blue CN-VOLETs compared with their respective OLEDs.

Device		Red	Green	Blue
		Turn-on voltage (V)		
CN-VOLET		−2.57	−2.52	−2.71
OLED		−2.60	−2.53	−2.81
	Luminance (cd/m^2)	Current efficiency (cd/A)		
CN-VOLET	250	12.5	48.0	23.3
OLED	250	12.4	49.8	23.9
CN-VOLET	500	12.1	47.2	22.8
OLED	500	12.3	48.3	23.1

Table 3. Comparison of effective aperture ratio and parasitic power dissipation percent between various OLED driving schemes.

Device*	Reference	Effective aperture ratio†	Parasitic power dissipation‡
TFT + OLED	(*8*)	50%	53%
MIS-OLET	(*18*)	45%	51%
CN-VOLET	This work	98%	6.2%

*All devices use the green phosphorescent emitter $Ir(ppy)_3$. †This parameter excludes the switching TFT and addressing lines (*19*). ‡Percentage of power dissipated across the driving transistor portion of the device not contributing to light generation; at 500 cd/m^2 display brightness (*30*).

2G) show highly uniform light emission across the 1 mm by 1 mm pixels.

To determine the performance losses incurred by the integrated drive transistor in the CN-VOLETs relative to simple OLEDs, we fabricated control OLEDs on ultraviolet-ozone–treated ITO in the same evaporation runs that deposited the OLED layers on the CN-VOLETs. Figure 3 compares the OLED and CN-VOLET devices. In all cases, the CN-VOLET gate voltage was −3 V. The CN-VOLETs all turn on (*29*) at voltages slightly below that of their corresponding OLED (Table 2).

By comparing the current efficiency (i.e., the amount of light emitted per unit of current) for each CN-VOLET to that of its corresponding control OLED, we can quantify the decrease in light output incurred by the integrated transistor layers in each of the devices. The current efficiency for each CN-VOLET and its corresponding OLED are plotted as a function of luminance in Fig. 3, D to F, as the drain voltage for the CN-VOLET and the cathode voltage for the OLED were each swept from 0 V to the terminal value of the sweep indicated at the arrow. As is evident there, the integrated transistor layers have a negligible effect on the current efficiency. Table 2 compares the current efficiencies of the CN-VOLET and OLED at moderate and high brightness. Averaging these values indicates that, for equal luminance, the CN-VOLET emits light with 98% the current efficiency of the control OLED. Because the CN-VOLET emits light across its entire face, the effective aperture ratio (*19*) of the CN-VOLET can rationally be taken to be 98%.

The control OLEDs can also be used to determine the parasitic power consumption of the integrated transistor layers in the CN-VOLETs. At a display brightness of 500 cd/m^2, the transistor elements account for only 19, 6, and 15% of the total power consumption in the red, green, and blue pixels, respectively. Published organic drive technologies that also used the green phosphorescent $Ir(ppy)_3$ emitter allow for a direct comparison (Table 3). At 500 cd/m^2 display brightness (*30*), the side-by-side TFT+OLED and the MIS-OLET exhibit a parasitic power consumption greater than 50% against the CN-VOLET's ~6%—more than a factor of 8 difference. Currents in our pixel off state are higher than would occur for a conventional lateral channel TFT driving an adjacent OLED, but any power saving there would quickly be overtaken by the lower on-state efficiency of the latter. Moreover, the off-state power consumption of our pixels remains quite small. The average off-state current densities of our devices (Fig. 2) is 1.7 $\mu A/cm^2$. For a −5.7 V average drain voltage (giving a bright on-state average luminance of 350 cd/m^2), this yields a power consumption for a 50-inch (127 cm) diagonal, 16:9 aspect ratio display, with every pixel in its off state, of 67 mW. For comparison, LCDs of this size consume 100 to 200 W, whether their pixels are on or off. Also listed in Table 3 are the effective aperture ratios (*19*) for the devices. The near-full aperture emission (~98%) of the CN-VOLET yields another major advantage: Because the integrated drive transistor of the CN-VOLET takes up no additional pixel area, the light emitter can occupy more of the pixel area, thereby achieving the same display brightness at substantially lower current density. This benefits OLED lifetime, which scales approximately as $1/J^2$, where J is the current density through the OLED (*9*).

References and Notes

1. G. Gu, S. R. Forrest, *IEEE J. Sel. Top. Quantum Electron.* **4**, 83 (1998).
2. M. J. Powell, *IEEE Trans. Electron. Dev.* **36**, 2753 (1989).
3. A. Nathan, G. R. Chaji, S. J. Ashtiani, *J. Display Technol.* **1**, 267 (2005).
4. M. J. Powell, C. Vanberkel, J. R. Hughes, *Appl. Phys. Lett.* **54**, 1323 (1989).
5. C.-P. Chang, Y.-C. S. Wu, *IEEE Electron Device Lett.* **30**, 1176 (2009).
6. Y. J. Park, M. H. Jung, S. H. Park, O. Kim, *Jpn. J. Appl. Phys.* **49**, 03CD01 (2010).
7. P.-S. Lin, T.-S. Li, *IEEE Electron Device Lett.* **15**, 138 (1994).
8. S. Ohta *et al.*, *Jpn. J. Appl. Phys. Part 1* **44**, 3678 (2005).
9. T. Tsujioka, H. Fujii, Y. Hamada, H. Takahashi, *Jpn. J. Appl. Phys. Part 1* **40**, 2523 (2001).
10. M. A. McCarthy, B. Liu, A. G. Rinzler, *Nano Lett.* **10**, 3467 (2010).
11. B. Liu *et al.*, *Adv. Mater. (Deerfield Beach Fla.)* **20**, 3605 (2008).
12. B. Park, H. Takezoe, *Appl. Phys. Lett.* **85**, 1280 (2004).
13. H. Iechi *et al.*, *Synth. Met.* **154**, 149 (2005).
14. K. Kudo, *Curr. Appl. Phys.* **5**, 337 (2005).
15. S. Y. Oh, H. J. Kim, S. K. Hwang, *Mol. Cryst. Liq. Cryst.* **458**, 247 (2006).
16. Z. Xu, S. H. Li, L. Ma, G. Li, Y. Yang, *Appl. Phys. Lett.* **91**, 092911 (2007).
17. H. Yamauchi, M. Iizuka, K. Kudo, *Jpn. J. Appl. Phys. Part 1* **46**, 2678 (2007).
18. K. Nakamura *et al.*, *Jpn. J. Appl. Phys.* **47**, 1889 (2008).
19. The effective aperture ratio is defined as the percent areal coverage of the light-emitting portion of the device compared to the total area occupied by the driving transistor, storage capacitor, and light emitter. For the MIS-OLET and CN-VOLET, the use of a storage capacitor is unnecessary due to the larger gate capacitance of the devices. This definition excludes the switching transistor and addressing lines (necessary components of any AMOLED display), allowing direct comparison of the relevant components of an AMOLED pixel that the CN-VOLET replaces.
20. C. Adachi, R. Kwong, S. R. Forrest, *Org. Electron.* **2**, 37 (2001).
21. Materials and methods are available as supporting material on *Science* Online.
22. T. Yamamoto, K. Takimiya, *J. Am. Chem. Soc.* **129**, 2224 (2007).
23. M. A. McCarthy *et al.*, *ACS Nano* **5**, 291 (2011).
24. T. Matsushima, C. Adachi, *J. Appl. Phys.* **103**, 034501 (2008).
25. S. Tokito, K. Noda, Y. Taga, *J. Phys. D Appl. Phys.* **29**, 2750 (1996).
26. M. Kimura *et al.*, *IEEE Trans. Electron. Dev.* **46**, 2282 (1999).
27. M. H. Jung, I. Choi, H. J. Chung, O. Kim, *Jpn. J. Appl. Phys.* **47**, 8275 (2008).
28. B. Liu, M. A. McCarthy, A. G. Rinzler, *Adv. Funct. Mater.* **20**, 3440 (2010).
29. The turn-on voltage is defined as the voltage at which the luminance surpasses 0.02 cd/m^2. This value is just above the off-state noise level measured by the Si photodiode used for the luminance measurements.
30. The display brightness (L_D) accounts for the limited emitting area of the OLED as defined by its effective aperture ratio (A). To achieve a given display brightness, the OLED must be driven at a larger luminance (L_O). The display brightness can be defined as $L_D = L_O \times A$.

Acknowledgments: We thank J. R. Reynolds (University of Florida) for useful discussions. We thank K. Takimiya (Hiroshima University) and E. Kanoh (Nippon Kayaku Co., Ltd.) for supplying the DNTT, and the University of Florida Nanoscale Research Facility for use of equipment and technical support. A portion of this research was conducted at the Center for Nanophase Materials Sciences, which is sponsored at Oak Ridge National Laboratory by the Scientific User Facilities Division, U.S. Department of Energy. We acknowledge support from the NSF (ECCS-0824157) and Nanoholdings LLC. The University of Florida has filed patent applications for the CN-VOLET architecture and for its use in AMOLED displays.

Supporting Online Material

www.sciencemag.org/cgi/content/full/332/6029/570/DC1
Materials and Methods
Figs. S1 to S5
Table S1
References

19 January 2011; accepted 24 March 2011
10.1126/science.1203052